

Application Note AN-EC-043

Studying PEDOT:PSS coatings with EQCM-D and Raman spectroscopy

EQCM-D with 3T analytik and Metrohm Autolab

PEDOT:PSS is an industrially relevant coating used in diverse fields such as energy, sensing, lighting, transparent electrodes, and wearable bioelectronics [1]. The coating properties are highly tunable, depending on factors like the counter-ion, secondary doping, and polymerization method.

This Application Note describes the use of EQCM-D (electrochemical quartz crystal microbalance with dissipation monitoring), Raman spectroscopy, and electrochemical measurements to investigate the synthesis of the PEDOT:PSS coating. Frequency and dissipation responses are recorded simultaneously across multiple harmonics and correlated in real time with electrochemical and Raman signals.

INTRODUCTION

When first synthesized, PEDOT was considered something of a breakthrough material as it can be easily electropolymerized from a solution of the EDOT monomer, forming a polymer of high conductivity (up to 200 S cm^{-1}, a value previously unseen). Adapting the polymerization process in the presence of PSSNa produces a conductive and highly stable polymer, appearing either transparent or dark blue depending on the thickness. PEDOT:PSS is now commercially available and continues to be studied for its unique properties.

SAMPLE AND EXPERIMENTAL DETAILS

The potentiostat/galvanostat used was a Metrohm Autolab AUT204 equipped with FRA32M module. The EQCM-D system was a 3T analytik eSorptionProbe OS. With this system, both the fundamental and several other overtone frequencies can be measured. The software packages used were NOVA, qGraph, and qGraph Viewer for associating the QCM-D and electrochemical data.

Part 1 – Electropolymerization

In the first part of this experiment, a PEDOT coating was deposited on the EQCM probe via constant current deposition. The parameters are listed in Table 1. Under these conditions EDOT is polymerized to PEDOT, and PSS is incorporated in the form of a charge-balancing counter-ion PSS^-.

Table 1. Parameters used in part 1 of this experiment.

Component	Details
Technique	Chronopotentiometry
Technique Parameter	80 µA, 150 seconds
Cell	Three-electrodes
Working Electrode	QCM Au crystal
Counter Electrode	Pt
Reference Electrode	Ag/AgCl
Electrolyte	0.01 mol/L EDOT, 0.1 mol/L $PSSNa^*$

In the literature, for PEDOT:PSS no large morphological differences have been found between constant current, potential, nor potentiodynamic deposition, therefore constant current was selected for ease of use [2]. Both were trialed in this study, and no large difference in the frequency or damping signal was seen. The frequency and damping signal were modelled in the qGraph Viewer software.

Part 2 – Coating assessment

In the second part of this experiment, the presence of PEDOT was confirmed via Raman spectroscopy and the capacitance of the polymer coating that was measured. The coating was washed with ultrapure water and then left to dry for 24 hours. The coated probe was then transferred to the DRP-RAMANCELL-M, and the cell filled with 0.1 mol/L KCl.

Raman spectroscopy was conducted with an i-Raman Plus 532H system with 100% laser power, 20 second integration time, and 3 time averaging. The capacitance of the coating was assessed by two different means: cyclic voltammetry (CV) and EIS (electrochemical impedance spectroscopy). For these measurements, the working electrode (WE) was the EQCM probe, the counter electrode (CE) was a Pt wire electrode, and the reference electrode (RE) was Ag/AgCl.

Cyclic voltammetry was conducted in the non-faradaic region between 0 and 0.4 V, at variable scan rates of 0.1, 0.05, 0.02, 0.005, and 0.001 V/s. The anodic and cathodic current at 0.2 V was extracted and plotted against the scan rate according to the following equation. The resulting slope of this graph is the capacitance of the electrode.

$$i = EDLC\ \frac{dV}{dt}$$

Here, i is the current, EDLC is the electric double layer capacitance, and dV/dt is the scan rate.

An alternative method to obtain the capacitance is EIS. Using this method, the capacitance was determined by measuring at the open circuit potential (OCP) in the frequency range of 10 kHz to 0.1 Hz, with an amplitude of 10 mV. Data above 1000 Hz was discarded due to the presence of reference electrode and inductance artifacts.

The remaining data was fitted to a simple equivalent circuit containing a resistor and constant phase element and the effective capacitance calculated from the following equation:

$$C_{eff}\,(F) = {Y_0}^{\frac{1}{n}} . \left(\frac{1}{R_s}\right)^{\frac{n-1}{n}}$$

Here, Y_0 is the CPE coefficient, n is the CPE exponent, and R_s is the series resistance.

RESULTS AND DISCUSSION

In Figure 1, the potential, frequency Δf, and damping ΔΓ signal as a function of time are shown. When the current is applied, the potential (in purple) rises rapidly to around 0.85 V—a potential that by CV is associated with the oxidation of the monomer EDOT to short-chain oligomers [3]. The potential falls slightly but reaches a steady state, consistent with the behavior seen in most constant current measurements. At the same time the frequency signal falls, signaling an increased mass at the working electrode. Across the full course of the experiment, Δf = -11,000 Hz, corresponding to a mass change per area density of around 48,000 ng/cm^2.

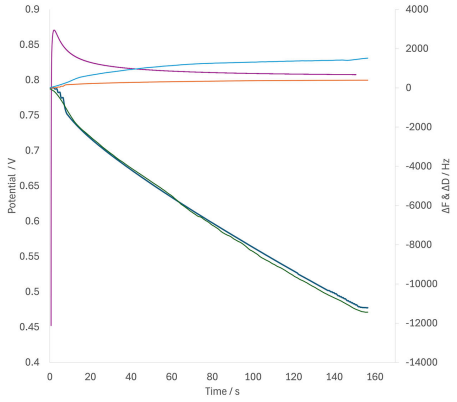


Figure 1. Potential (purple), frequency (dark green – fundamental, light green – F3 overtone), and damping (orange – fundamental, blue – F3 overtone) signals recorded during the course of the deposition.

Two regions of this signal response can be identified, one in the first 10–20 seconds of the deposition where the reaction is more likely to be associated with the oxidation of the monomer and its conversion to short chain oligomers [3]. Here the fall in frequency and rise in damping happens more rapidly. The second region is noted at a certain point where the oligomers begin to polymerize and the mass thereafter increases at a stable rate, remaining consistent throughout the rest of the deposition. Simultaneously, the rise in damping becomes slower over time.

To investigate dynamic changes in the mechanical properties of the deposited layer, the change in damping relative to frequency (ΔΓ/Δf-ratio) was plotted as a function of time in Figure 2. The ΔΓ/Δf-ratio rapidly increases to a value of about 0.25 at the onset of monomer oxidation to short-chained oligomer. This indicates that the oligomer layer is viscoelastic in nature. Soon after, coinciding with oligomer polymerization, the ΔΓ/Δf-ratio rapidly drops to values below 0.1, and continues dropping henceforth.

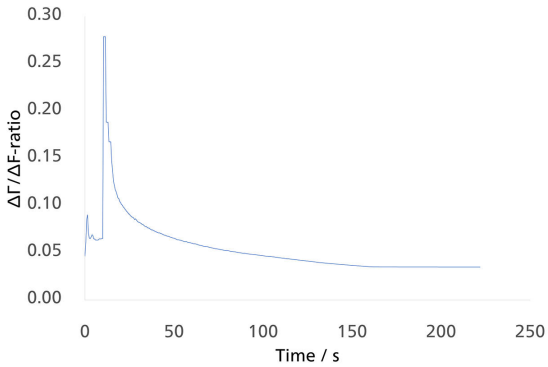


Figure 2. ΔΓ/Δf-ratio of the fundamental frequency over the course of the experiments. The initial rapid increase to ratios of 0.25 followed by a rapid but gradual drop over time indicates that the layer stiffens as polymerization occurs.

Damping signals >10% of the frequency shift is a key indication that a layer has viscoelastic properties [4]. Such layers require viscoelastic modelling tools (also provided in qGraph Viewer) for precise calculation of layer thickness.

In this case, however, the damping drops to well below 10% of the frequency shift during PEDOT:PSS polymerization. This indicates that the final polymer layer is rigid and that the Sauerbrey equation (shown here) applies.

$\Delta\phi = -C_f \cdot \Delta f$

Here, C_f = 4.3 ng · cm^{-2} · Hz^{-1} is the sensitivity coefficient for this crystal, and $\Delta\phi = \Delta m / A_q$ represents the area density. The layer thickness can then be calculated by dividing $\Delta\phi$ by the material density ρ.

A dedicated tool for this exists in qGraph Viewer. A density of 1.011 g cm^{-3} was used for the layer thickness calculation, which is the density provided for dried coating of the commercially available PEDOT:PSS by Sigma-Aldrich. The qGraph Viewer software estimates a total thickness of the layer at 474–486 nm, using Δf1 and Δf3, respectively.

In the second part of the experiment, following washing, mounting in a Raman cell, and immersion of the EQCM probe in KCl, the Raman spectrum shown in Figure 3 was collected.

The Raman spectrum unambiguously confirms the presence of PEDOT at the electrode surface, with the bands higher than 1000 cm^{-1} being particularly relevant for this. The highest intensity peak, i.e., at ~1430 cm^{-1}, has historically been used to guide doping of the polymer film as the red and blue shift of this band corresponds well with changes in the electronic structure of the polymer [5]. A full list of the Raman shifts of each band and its assignment is given in Table 2.

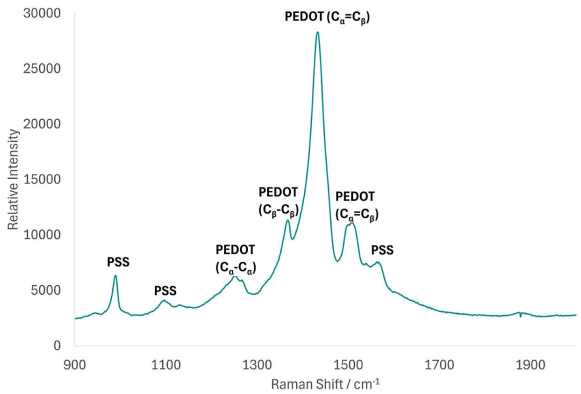


Figure 3. Raman spectrum of the coated electrode, confirming presence of PEDOT:PSS.

Table 2. Raman band assignments and Raman shift [5].

Assignment	Wavenumber / cm^{-1}
PSS	990
PSS	1097
PEDOT (C_α-C_α)	1255
PEDOT (C_β-C_β)	1369
PEDOT (C_α=C_β)	1430
PEDOT (C_α=C_β)	1502
PSS	1568

The capacitance of the coated electrode was also calculated from two methods and compared to that of the bare electrode. In Figure 4, the CV in the non-faradaic region is shown. From this, the anodic and cathodic currents at 0.2 V for each scan rate were extracted and plotted against the scan rate. The slopes of these lines give the capacitance directly and in each case was ~700 µF.

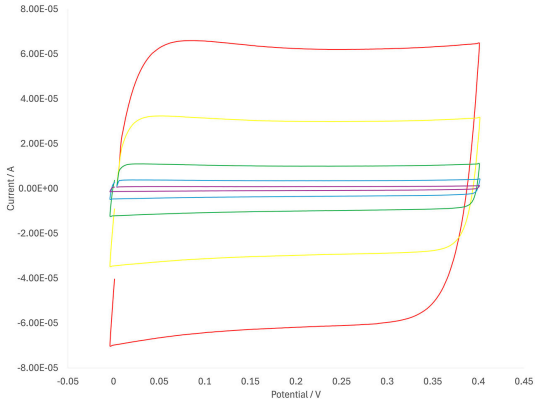


Figure 4. CV in the non-faradaic region shown for the coated electrode at various scan rates.

The Nyquist and Bode plots of the coated electrode are shown in Figures 5a and 5b. These plots indicate R-C serial (resistor-capacitor) type behavior and are thus consistent with an intact coating. A constant phase element was actually used to model the non-ideality of the capacitance. The effective capacitance was extracted using the equation shown earlier and was calculated at around 710 µF. The consistency between these two values grants confidence in the two methods. The EIS method was used to obtain the capacitance of the bare electrode and was calculated at 80 µF.

The close to eight-fold increase in the capacitance upon coating the electrode is consistent with the pseudo-capacitive nature of this polymer, as well as the general increase in the effective electrochemical surface area (roughness) that comes with coating an electrode [1].

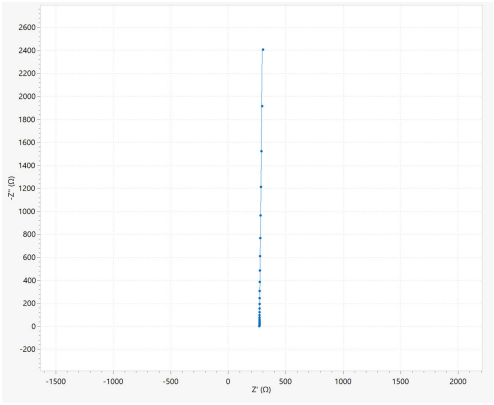


Figure 5a. Nyquist plot of the coated electrode in the frequency range of 1000 to 0.1 Hz.

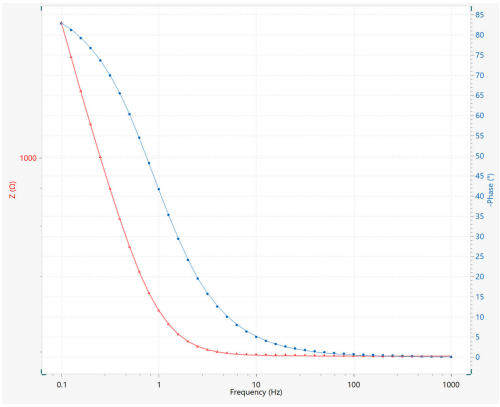


Figure 5b. Bode plot of the coated electrode in the frequency range of 1000 to 0.1 Hz.

CONCLUSIONS

This Application Note introduced a novel probe-based system for EQCM-D analysis of an industrially relevant polymer coating (PEDOT:PSS). EQCM-D has been shown to be highly effective in aiding the design and optimization of this type of coating, and this probe-based system affords the additional chance to obtain Raman spectra in situ. The system is therefore a powerful aid for researchers working in this field.

REFERENCES

1. Gueye, M. N.; Carella, A.; Faure-Vincent, J.; et al. Progress in Understanding Structure and Transport Properties of PEDOT-Based Materials: A Critical Review. *Progress in Materials Science* **2020**, *108*, 100616. DOI:10.1016/j.pmatsci.2019.100616
2. Boz, E. B.; Fritz, M.; Forner-Cuenca, A. Electropolymerized Poly(3,4-Ethylenedioxythiophene) Coatings on Porous Carbon Electrodes for Electrochemical Separation of Metals. *Advanced Materials Interfaces* **2023**, *10* (9), 2202497. DOI:10.1002/admi.202202497
3. Pigani, L.; Heras, A.; Colina, Á.; et al Electropolymerisation of 3,4-Ethylenedioxythiophene in Aqueous Solutions. *Electrochemistry Communications* **2004**, *6* (11), 1192–1198. DOI:10.1016/j.elecom.2004.09.021
4. Easley, A. D.; Ma, T.; Eneh, C. I.; et al. A Practical Guide to Quartz Crystal Microbalance with Dissipation Monitoring of Thin Polymer Films. *Journal of Polymer Science* **2022**, *60* (7), 1090–1107. DOI:10.1002/pol.20210324
5. Culebras, M.; Gómez, C. M.; Cantarero, A. Enhanced Thermoelectric Performance of PEDOT with Different Counter-Ions Optimized by Chemical Reduction. *J. Mater. Chem. A* **2014**, *2* (26), 10109–10115. DOI:10.1039/C4TA01012D

CONTACT

บริษัท เมทโธรห์ม สยาม จำกัด
979 111-115 อาคาร S.M.
Tower ชั้น33, แขวงพญาไท,
เขตพญาไท, ถ.พหลโยธิน
กรุงเทพมหานคร 10400
info@metrohm.co.th

CONFIGURATION



Autolab PGSTAT204

The PGSTAT204 combines the small footprint with a modular design. The instrument includes a base potentiostat/galvanostat with a compliance voltage of 20 V and a maximum current of 400 mA or 10 A in combination with the BOOSTER10A. The potentiostat can be expanded at any time with one additional module, for example the FRA32M electrochemical impedance spectroscopy (EIS) module.

The PGSTAT204 is an affordable instrument which can be located anywhere in the lab. Analog and digital inputs/outputs are available to control Autolab accessories and external devices are available. The PGSTAT204 includes a built-in analog integrator. In combination with the powerful NOVA software it can be used for most of the standard electrochemical techniques.



i-Raman Plus 532H Portable Raman Spectrometer

The i-Raman® Plus 532H is part of our award-winning series of i-Raman portable Raman spectrometers powered by our innovative intelligent spectrometer technology. Using a high-quantum-efficiency CCD array detector with TE cooling and high dynamic range, this portable Raman spectrometer delivers excellent performance with low noise, even at integration times of up to 30 minutes, making it possible to measure weak Raman signals.

The i-Raman Plus 532H features the unique combination of wide spectral range and high resolution with configurations which allow measurements from 65 cm^{-1} to 3,400 cm^{-1}. The system's small footprint, lightweight design, and low power consumption ensure research-grade Raman analysis capabilities at any location. The i-Raman Plus is equipped with a fiber probe for easy sampling, and can be used with a cuvette holder, a video microscope, an XYZ positioning stage with a probe holder, as well as our proprietary BWIQ® multivariate analysis software and BWID® identification software. With the i-Raman Plus, you always have a high precision Raman solution for qualitative and quantitative analysis.